EUKARYOTIC CELL, Feb. 2005, p. 379–391 Vol. 4, No. 2
1535-9778/05/$08.00+0 doi:10.1128/EC.4.2.379–391.2005

The High-Mobility-Group Domain Transcription Factor Rop1 Is a Direct Regulator of *prf1* in *Ustilago maydis*

Thomas Brefort, Philip Müller, and Regine Kahmann*

Max Planck Institute for Terrestrial Microbiology, Marburg, Germany

Received 4 August 2004/Accepted 18 November 2004

In the smut fungus *Ustilago maydis*, the pheromone signal is transmitted via a mitogen-activated protein kinase module to the high-mobility-group (HMG) domain transcription factor Prf1, leading to its activation. This triggers sexual and pathogenic development since Prf1 binds to the PRE boxes located in the promoters of the *a* and *b* mating type genes. Here, we present the characterization of *rop1* and *hmg3*, encoding two additional sequence-specific HMG domain proteins. While *hmg3* mutants are slightly impaired in mating and do form conjugation hyphae, *rop1* deletion strains display a severe mating and filamentation defect and do not respond to pheromone stimulation. In particular, *rop1* is essential for pheromone-induced gene expression in axenic culture. Constitutive expression of *prf1* fully complements the mating defect of *rop1* mutants, indicating that *rop1* is required for *prf1* gene expression. Indeed, we could show that Rop1 binds directly to specific elements in the *prf1* promoter. Surprisingly, on the plant surface, *rop1* deletion strains do form conjugation hyphae and express sufficient amounts of *prf1* to cause full pathogenicity. This indicates the involvement of additional components in the regulation of *prf1* gene expression during pathogenic growth.

The high-mobility-group (HMG) box superfamily of transcription factors is defined by conserved DNA-binding domains. Based on primary sequence and DNA-binding characteristics, this class of proteins is divided into two major subfamilies. One of these subfamilies includes proteins with multiple HMG boxes exemplified by the HMG-1 and HMG-2 proteins, which have a rather nonspecific affinity for DNA (11, 17, 30). The second subfamily consists of proteins with a single HMG domain, which binds sequence-specifically to variants with the consensus motif (A/T)(A/T)CAAAG (52). Members of this subfamily are important regulators of diverse differentiation processes, including the mammalian sex-determining factor SRY (44), the related SOX proteins (40), and the lymphoid-specific transcription factors LEF-1 and TCF-1 (49). In yeasts and fungi, HMG box proteins of this class are especially involved in sexual differentiation. Examples are Mat-Mc and Ste11 from *Schizosaccharomyces pombe*, which determine mating type and control conjugation as well as sporulation, respectively (27, 46), Pcc1 in *Coprinus cinereus*, which functions as a repressor of A-regulated sexual morphogenesis (38), and Prf1 in *Ustilago maydis*, an essential factor for sexual and pathogenic development (18).

In *U. maydis*, the causative agent of corn smut disease, fusion of compatible partners is genetically controlled by the biallelic *a* locus, encoding pheromone (*mfa1*/*2*) and receptor (*pra1*/*2*) genes (6). Subsequent filamentous growth and pathogenic development are regulated by the multiallelic *b* locus (4). This locus codes for two homeodomain proteins, bE and bW, which dimerize to generate an active transcription factor when derived from different alleles (16, 24). Basal as well as pheromone-induced transcription of the genes in the *a* and *b* loci is regulated by the HMG box protein Prf1, which binds to pheromone response elements (PREs) present in the regulatory regions of the *a* and *b* mating type genes (18, 51). Consequently, *prf1* deletion mutants are sterile and nonpathogenic.

To perform its function, Prf1 needs to be activated through both a conserved mitogen-activated protein (MAP) kinase module consisting of Kpp4/Ubc4 (MAPKKK), Fuz7/Ubc5 (MAPKK), and Kpp2/Ubc3 (MAP kinase) (1, 4, 22, 35–37) and a conserved cyclic AMP (cAMP) signaling pathway (29, 41). Activation of the MAP kinase cascade results in *prf1*-dependent gene expression, and among the genes whose transcription is activated are *prf1* itself, *mfa*, *pra*, *bE*, and *bW* (18, 51). In addition, the cAMP pathway triggers pheromone-responsive expression of these genes (29, 41). Cross talk between protein kinase A and MAP kinase signaling during mating is mediated by the posttranscriptional modification of Prf1 at protein kinase A as well as MAP kinase phosphorylation sites (22).

Recent experiments have indicated that the signaling pathway bifurcates downstream of the MAP kinase Kpp2. One branch leads to the described transcriptional responses, and all of these require Prf1 (18, 37). The other branch triggers conjugation tube formation, and this morphological transition is independent of *prf1* (37). In addition to posttranscriptional regulation, *prf1* is regulated on the transcriptional level by an upstream activating sequence (UAS) located in its promoter (19). The UAS determines expression through environmental signals (e.g., nutrients). Furthermore, two PRE boxes in the *prf1* promoter are probably involved in the autoregulation of *prf1* transcription.

In this study, we have investigated the roles of additional HMG domain proteins in *U. maydis* development. We describe the characterization of *rop1* in detail, which turned out to be a transcriptional regulator of *prf1* exclusively during axenic growth.

* Corresponding author. Mailing address: Max Planck Institute for Terrestrial Microbiology, Karl-von-Frisch-Strasse, D-35043 Marburg, Germany. Phone: 49-6421-178-501. Fax: 49-6421-178-509. E-mail: kahmann@staff.uni-marburg.de.

TABLE 1. *U. maydis* strains used in this study

Strain	Reference	Plasmid transformed	Integration locus	Progenitor strain
FB1 (*a1 b1*)	3			
FB2 (*a2 b2*)	3			
SG200 (*a1:mfa2 bE1 bW2*)	5			
CL13 (*a1 bE1 bW2*)	5			
FB1P_{crg1}:fuz7DD	37			
FB1Δkpp2-1P_{crg1}:fuz7DD	37			
FB1Δprf1P_{crg1}:fuz7DD	37			
HA232 (*a2 b2 B-UAS3$_{prf1}$:ip*)	19			
FB1Δrop1	This study	pΔrop1-hyg	*rop1*	FB1
FB2Δrop1	This study	pΔrop1-hyg	*rop1*	FB2
SG200Δrop1	This study	pΔrop1-hyg	*rop1*	SG200
HA232Δrop1	This study	pΔrop1-hyg	*rop1*	HA232
FB1Δhmg3	This study	pΔhmg3-nat	*hmg3*	FB1
FB2Δhmg3	This study	pΔhmg3-nat	*hmg3*	FB2
SG200Δhmg3	This study	pΔhmg3-nat	*hmg3*	SG200
FB1Δrop1P_{crg1}:fuz7DD	This study	pΔrop1-hyg	*rop1*	FB1P_{crg1}:fuz7DD
FB1Δrop1Δprf1P_{crg1}:fuz7DD	This study	pΔrop1-hyg	*rop1*	FB1Δprf1P_{crg1}:fuz7DD
FB1Δhmg3P_{crg1}:fuz7DD	This study	pΔhmg3-nat	*hmg3*	FB1P_{crg1}:fuz7DD
FB1Δhmg3Δrop1P_{crg1}:fuz7DD	This study	pΔhmg3-nat	*hmg3*	FB1Δrop1P_{crg1}:fuz7DD
FB1Δrop1prf1^{con}	This study	pPRF1^{con}	*prf1*	FB1Δrop1
FB2Δrop1prf1^{con}	This study	pPRF1^{con}	*prf1*	FB2Δrop1
FB2Δrop1P_{otef}:rop1	This study	p123P_{otef}:rop1	*ip*	FB2Δrop1
SG200Δrop1P_{otef}:rop1	This study	p123P_{otef}:rop1	*ip*	SG200Δrop1
FB1P_{prf1}:gfp	This study	pP_{prf1}-1746:gfp	*ip*	FB1
FB2P_{prf1}:gfp	This study	pP_{prf1}-1746:gfp	*ip*	FB2
FB1Δrop1P_{prf1}:gfp	This study	pP_{prf1}-1746:gfp	*ip*	FB1Δrop1
FB2Δrop1P_{prf1}:gfp	This study	pP_{prf1}-1746:gfp	*ip*	FB2Δrop1

MATERIALS AND METHODS

Strains and growth conditions. The *Escherichia coli* K-12 derivatives DH5α (Bethesda Research Laboratories) and Top10 (Invitrogen) were used for cloning purposes, and *E. coli* Rosetta(DE3)(pLysS) (Novagen) was used for protein expression. The *U. maydis* strains used in this study are listed in Table 1. *U. maydis* strains were grown as indicated at 28°C in liquid complete medium (CM) (21), nitrate minimal medium (NM) supplemented with either 1% glucose or 1% maltose (19), YEPSL (0.4% yeast extract, 0.4% peptone, 2% sucrose), or potato dextrose (PD) (2.4% PD broth [Difco]) medium or solid PD agar. For induction of the *crg1* promoter, strains were grown in CM medium containing 1% glucose to an optical density at 600 nm (OD_{600}) of 0.5, washed twice with water, resuspended in CM medium with 1% arabinose as a carbon source, and grown for the time indicated in each experiment.

Hygromycin B was from Roche (Pensberg, Germany), nourseothricin (ClonNAT) was obtained from the Hans Knöll Institute (Jena, Germany), and carboxin was from Riedel de Haen (Seelze, Germany). All other chemicals were of analytical grade and were obtained from Sigma or Merck.

Plasmids and plasmid construction. Plasmids pTZ19R (Pharmacia), pSP72 (Promega), pSL1180 (Pharmacia), and pBS(+)SKII (Stratagene) were used for cloning, subcloning, and sequencing of genomic fragments, and pCR2.1TOPO (Invitrogen) was used for cloning and sequencing of fragments generated by PCR. pET15b (Novagen) was used for protein expression in *E. coli*. Sequence analysis of genomic fragments and fragments generated by PCR was performed with an automated sequencer (ABI 377) and standard bioinformatic tools.

pMF1h contains a hygromycin resistance cassette as an SfiI fragment, and pMF1n contains a nourseothricin resistance cassette as an SfiI fragment (8). p123 is a pSP72 derivative containing the enhanced green fluorescent protein (EGFP) gene *egfp* (Clontech) fused to the *otef* promoter, an *nos* terminator, and a carboxin resistance cassette (53). pCU4 codes for carboxin resistance and carries the *gfp* gene under the control of the constitutive *otef* promoter (33); pAH298HMG is a pET15b derivative for the heterologous expression of the HMG domain of Prf1 comprising amino acids 1 to 289 as an N-terminally 6xHis-tagged fusion protein (18).

To isolate the *hmg3* gene, a 0.77-kb PCR fragment was generated with primers hmg3uni1 (GCGGCATCAGAGCATCG) and hmg3rev2 (GGACTCAGAAGC ATCGGC). The amplified *hmg3* fragment was used to screen a genomic cosmid library (43). A 3.3-kb region of the hybridizing cosmid 20C9, comprising the *hmg3* open reading frame, was sequenced.

The *rop1* gene was subcloned from a genomic bacterial artificial chromosome library (LionBioscience) as a 7.7-kb SacII fragment into the SacII site of pBS(+)SKII, and the resulting plasmid was designated pRop1-7.7S.

cDNA of *rop1* was isolated from a λgt10 cDNA library (6) by PCR. The PCR fragments were cloned in pCR2.1-TOPO to yield pTB20 to pTB25 and sequenced.

Deletion constructs were generated according to Kämper (23). In particular, for pΔrop1-hyg, a 1.1-kb fragment comprising the 5′ flank and a 1.0-kb fragment comprising the 3′ flank of the *rop1* open reading frame were generated by PCR on *U. maydis* FB1 DNA with primer combinations OTB27L (CATTCCCTTTC GTCGTCCTTGATC)-OTB28L2 (CACGGCTGAGTGGCCTGAAGCAGTC AAATCACGCCAGG) and OTB15R1 (GTGGGCCATCTAGGCCGCACTG AAGTCTTGACACAGATGC)-OTB16R2 (GGTCAGTACTTGATACTAAG CGCC), respectively. These fragments were then digested with SfiI and ligated to the 2.7-kb SfiI hygromycin resistance cassette from pMF1-h (8). The resulting ligation products were cloned into pCR2.1-TOPO. This plasmid, p*Δrop1*-hyg, was subsequently used as a template to amplify the *rop1* deletion construct with primers OTB27L and OTB16R2.

To generate pΔhmg3-nat, a 1.0-kb fragment comprising the 5′ flank and a 1.0-kb fragment comprising the *hmg3* 3′ region from bp 1713 to 2663 were generated by PCR on *U. maydis* FB1 DNA with primer combinations L152uni (CGACTTGGAGAAGTGCGCG)-L152SfiIrev (ACACGGCCTGAGTGGCC TAGCGAGATGGAGTTGGGGC) and R152SfiIuni (TGTGGGCCATCTAG GCCCGGCGCGAATCAAGTACAGAGC)-R152rev (GCGATGAGTTTGGC GAGACGG), respectively. These fragments were then digested with SfiI and ligated to the 1.4-kb SfiI nourseothricin resistance cassette from pMF1n (8). The resulting ligation products were cloned into pCR2.1-TOPO to yield pΔhmg3-nat. This plasmid was subsequently used as a template to amplify the *hmg3* deletion construct with primers L152uni and R152rev.

Plasmid p123P_{otef}:rop1 was constructed by replacing the 0.7-kb NcoI-NotI *egfp* gene fragment of p123 with a 2.2-kb NcoI-HindIII fragment from pET15bRop1 (see below) coding for the N-terminally 6xHis-tagged version of Rop1. p123P_{otef}:*rop1* carries the *6xHis*::*rop1* allele under the control of the constitutive *otef* promoter.

In pPprf1−1746:*gfp*, the *prf1* gene promoter up to position −1746 is ligated to the *gfp* gene. To yield this plasmid, the *otef* promoter in pCU4 (33) was replaced by the *prf1* promoter.

pET15bRop1 was constructed by ligating a 1.8-kb SalI-BglII-digested PCR

product generated with primers Rop1-5′SalI (GTCGACATGGCGCAACAGG GCTATGGC) and Rop1-3′BglII (AGATCTTCAGTGCCCAGAGGCGC) encompassing the complete *rop1* open reading frame into the XhoI and BamHI sites of pET15b to yield a translational *6xHis*::*rop1* fusion at the N terminus of *rop1*.

pET15bHMGRop1 was constructed by ligating a 0.91-kb SalI- and BglII-digested PCR product generated with primers Rop1HMG-5′SalI (GTCGACC TGTCCAATCATCCGACC) and Rop1HMG-3′BglII (AGATCTGTGTTGCA AGTTCGCCACG) encoding the HMG domain of Rop1 (amino acids 100 to 401 of the protein) into the XhoI and BamHI sites of pET15b to yield a translational *6xHis*::$rop1_{100\text{-}401}$ fusion.

For transformation into *U. maydis*, linear deletion constructs were generated from the deletion plasmids by PCR; $pPRF1^{con}$ (19) was digested with DraI, and plasmids $p123P_{otef}$:rop1 and pPprf1−1746:gfp were linearized with SspI prior to transformation. In all cases, single homologous integration events into the respective loci were verified by Southern analysis.

DNA and RNA procedures. Standard molecular techniques were used for DNA and RNA procedures (42). Transformation of *U. maydis* was performed as published previously (43). *U. maydis* DNA was isolated as described (20). RNA from strains grown in liquid culture was prepared as described (29) or following the Trizol reagent protocol (Invitrogen). The following probes were used for Northern analyses: a 0.67-kb EcoRV fragment and a 1.3-kb EcoRI-EcoRV fragment from pSP4.2EcoRV (6) for *mfa1* and *pra1*, respectively; a 2.6-kb PvuII fragment from pbW2-Nde-bE1 (10) for *bE* and *bW*; and a 1.6-kb EcoRV fragment from pRF-6.0B (19) for *prf1*. For *rop1*, a 0.2-kb fragment was generated with primers OTB9 (ACCTCGGCCACCTAATGC) and OTB12 (GGCGATA TCGGTAGGTGG) by PCR on FB1 DNA. For *hmg3*, a 0.77-kb PCR product generated with primers hmg3uni1 and hmg3rev2 (see above) was used. Radioactive labeling was performed with the NEBlot kit (New England Biolabs). A 5′-end-labeled oligonucleotide complementary to the *U. maydis* 18S rRNA was hybridized as a loading control in Northern analyses (7). For visualization and quantification of radioactive signals, a PhosphorImager (Storm 840; Molecular Dynamics) and the program ImageQuant (Molecular Dynamics) were used.

Mating, pheromone stimulation, and pathogenicity assay. To test for mating, compatible strains were cospotted on charcoal-containing PD plates (21), and the plates were sealed with Parafilm and incubated at 28°C for 48 h. For pheromone stimulation, strains were grown in CM with 1% glucose to an OD_{600} of 0.6. Synthetic pheromone (kindly provided by M. Tönnies and H. Kessler) dissolved in dimethyl sulfoxide was added to a final concentration of 2.5 μg/ml, and cells were harvested for microscopic observations and RNA preparations after 5 h of incubation in a 15-ml plastic tube on a tissue culture roller at 28°C.

Plant infections of the corn variety Early Golden Bantam (Olds Seeds, Madison, Wis.) were performed as described previously (36). Fungal structures on the plant surface were visualized by Calcofluor staining as described previously (9).

Fluorimetric measurement of GFP. Cells grown in NM plus 1% glucose or 1% maltose to an OD_{600} of 0.5 to 0.8 were pelleted and resuspended in sterile H_2O to an OD_{600} of 1.0; 200 μl of cell suspension was transferred to a microtiter plate, and fluorescence was measured in a Tecan Saphire fluorescence reader. GFP fluorescence was measured at a wavelength of 485 nm for excitation and 520 nm for emission, with a bandwidth of 7.5 nm in both cases. Fluorescence was normalized to the OD_{600} (22). At least two independent cultures were scored, and each was measured in triplicate to yield mean values.

Protein expression and purification and electrophoretic mobility shift assays. Rosetta(DE3)(pLysS) cells containing plasmid pET15bHMGRop1 or pAH289HMG (18) were grown in dYT (1.6% trypto-peptone, 1% yeast extract, 0.5% NaCl) containing 1% glucose, ampicillin (100 μg/ml), and chloramphenicol (34 μg/ml) at 37°C. At an OD_{600} of ≈0.5, cells were shifted to 20°C, and expression was induced by the addition of 0.1 mM isopropylthiogalactopyranoside (IPTG). After overnight incubation, cells were harvested and resuspended in buffer A (20 mM Tris, pH 7.9, 0.5 M NaCl, 5 mM imidazole, 0.1 mM Triton X-100, and complete protease inhibitor cocktail [Roche]). All subsequent steps were performed on ice or at 4°C. Cells were disrupted by five passages through a French pressure cell (Minicell, 20,000 lb/in2). After centrifugation (13,000 × *g*, 1 h, 4°C) the cleared lysates were subjected to Ni-NTA affinity chromatography (Ni-nitrilotriacetic acid resin, Qiagen) according to the manufacturer's protocol. For washing steps, buffer A containing 60 mM imidazole was used, and elution was performed with buffer A containing 1 M imidazole. The purified His-tagged HMG domains of Rop1 and Prf1 ($Rop1_{100\text{-}401}$ and $Prf1_{1\text{-}289}$ proteins, respectively) were desalted on PD10 columns (Pharmacia) with retention buffer (25 mM HEPES, pH 7.9, 100 mM KCl, 1 mM EDTA, 1 mM dithiothreitol, 10% glycerol, and complete protease inhibitor cocktail; see above) for elution. Fractions (0.5 ml) were collected and assayed for protein content and purity by sodium dodecyl sulfate-polyacrylamide gel electrophoresis and staining with Coomassie blue.

Electrophoretic mobility shift assays were performed with 100 to 200 ng of purified $Rop1_{100\text{-}401}$ or $Prf1_{1\text{-}289}$ protein in retention buffer (see above) supplemented with 1 μg of bovine serum albumin and 0.4 μg of poly(dI-dC) in a total volume of 10 μl. Samples were incubated for 20 min at room temperature, ^{32}P-labeled probe (10,000 cpm) was added, and incubation was continued for 30 min. For competition experiments, unlabeled probes were added after 10 min of incubation, and labeled probes were introduced after further incubation for 10 min.

The probes used for the experiments were consecutive (fragments a to e in Fig. 6) and overlapping restriction fragments (a1 and a2 and d1 and d2, Fig. 6) of the *prf1* promoter generated by digests of plasmid pRF-6.0B (19). Fragment a is a 438-bp SphI-XhoI fragment; fragment b is a 413-bp XhoI-NdeI fragment; fragment c is a 366-bp NdeI-NspI fragment; fragment d is a 454-bp NspI-XbaI fragment; fragment e is a 427-bp XbaI-SalI fragment; fragment a1 is a 282-bp SphI-NcoI fragment; fragment a2 is a 276-bp NspI-XhoI fragment; fragment d1 is a 268-bp NspI-BpmI fragment; and fragment d2 is a 228-bp SacII-XbaI fragment. In addition, three pairs of complementary oligonucleotides were annealed to yield three double-stranded 33-bp probes with single-base 5′ overhangs: PREuni (CAAATCTGTGAATCCCTTTGTGCCAGTTGACTG) annealed to PRErev (GCAGTCAACTGGCACAAAGGGATTCACAGATTT); RRS2uni (TGCAACCGACTTATTGTCCTTTCCCGAACTCCA) annealed to RRS2rev (TTGGAGTTCGGGAAAGGACAATAAGTCGGTTGC); and RRSm-uni (A TCACCATCACCCGGTGAGGGGCACCAGCGCGC) annealed to RRSm-rev (AGCGCGCTGGTGCCCCTCACCGGGTGATGGTGA). Equimolar amounts of the DNA fragments were 5′-end labeled by T4 polynucleotide kinase (New England Biolabs) and [γ-^{32}P]ATP (6,000 Ci/mmol) according to the manufacturer's instructions.

Protein-DNA complexes were separated in polyacrylamide gels (4%) in 0.5x Tris-borate-EDTA buffer at 9 mA per gel for 1 to 3 h, depending on probe size. Gels were dried, and radioactive probes and complexes were visualized by PhosphorImager analysis (Molecular Dynamics).

Microscopic observation. For microscopic observation, a Zeiss Axiophot microscope with differential interference contrast optics was used. Calcofluor fluorescence was observed with a standard DAPI (4′,6′-diamidino-2-phenylindole) filter set. GFP fluorescence was detected with a specific filter set (BP 470/20, FT493, BP 505 to 530; Zeiss, Jena, Germany). Pictures were taken with a charge-coupled device camera (Hamamatsu, Herrsching, Germany). Image processing was done with Image Pro (Media Cybernetics), Adobe Photoshop 6.0, and Canvas 6.0 (Deneba Systems).

Nucleotide sequence accession numbers. The GenBank accession numbers for *rop1* and *hmg3* are AY677184 and AY677183, respectively.

RESULTS

Identification of additional HMG domain proteins encoded by *U. maydis*. As the HMG box transcription factor Prf1 is essential for mating but not required for the process of conjugation tube formation (37), we were interested in identifying additional transcription factors encoded by the *U. maydis* genome which may control this morphogenetic process. In the human pathogens *Cryptococcus neoformans* and *Candida albicans* as well as in the phytopathogen *Magnaporthe grisea* Ste12-like homeodomain proteins are important for filamentous growth and virulence (12, 31, 32, 39, 55, 56). However, we were not able to identify an open reading frame coding for an Ste12-like protein in the *U. maydis* genome. Therefore, we concentrated on the HMG box family of transcriptional regulators as such factors are known to be involved in the regulation of sexual development in fungi. When highly conserved HMG DNA-binding domains were used to screen the *U. maydis* genome sequence, seven predicted open reading frames coding for potential HMG domain proteins were identified besides Prf1. One of these predicted open reading frames contains two HMG boxes (Fig. 1A, 48_420.A, and 48_420.B). While the HMG domains of two proteins, termed Rop1 and

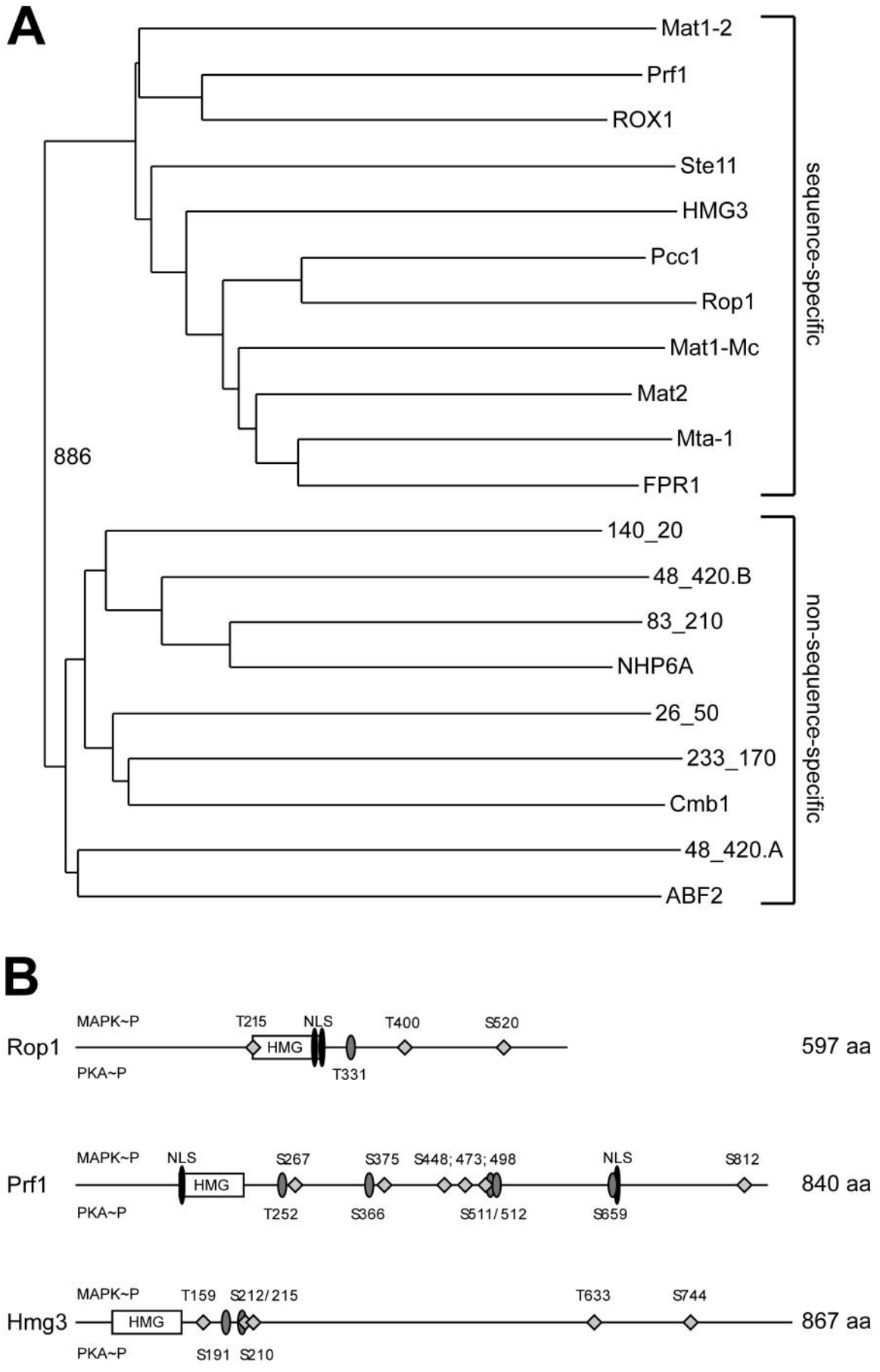
A
Mat1-2
Prf1
ROX1
Ste11
HMG3
Pcc1
Rop1
Mat1-Mc
Mat2
Mta-1
FPR1
886
sequence-specific
140_20
48_420.B
83_210
NHP6A
26_50
233_170
Cmb1
48_420.A
ABF2
non-sequence-specific
B
Rop1
MAPK~P
PKA~P
T215
NLS
HMG
T331
T400
S520
597 aa
Prf1
MAPK~P
PKA~P
NLS
HMG
S267
T252
S375
S366
S448; 473; 498
S511/512
NLS
S659
S812
840 aa
Hmg3
MAPK~P
PKA~P
HMG
T159
S212/215
S191
S210
T633
S744
867 aa

Hmg3, clustered with the sequence-specific class (Fig. 1A), the other six belonged to the non-sequence-specific class (Fig. 1A).

We focused on the two putative sequence-specific HMG domain proteins Rop1 and Hmg3. The *rop1* open reading frame comprises 2,778 bp. cDNA analysis revealed two introns of 462 bp and 441 bp. The HMG domain encoded by *rop1* (amino acids 216 to 296) shows closest homology to Pcc1 of *Coprinus cinereus*, a negative regulator of pseudoclamp formation (38) (Fig. 1A). The deduced amino acid sequence of Rop1 is predicted to contain two putative nuclear localization signals (http://psort.nibb.jp) located between amino acids 282 and 296 and three potential MAP kinase sites of the consensus L/PXS/TP (13) (Fig. 1B). In addition, one potential protein kinase A phosphorylation site is predicted at amino acid position 331 (http://www.expasy.org/cgi-bin/scanprosite) (Fig. 1B).

The HMG domain of Hmg3 shows closest homology to Mat2 from *Gibberella fujikuroi*. The intronless *hmg3* gene comprises 2,604 bp and codes for a protein of 867 amino acids that is predicted to be localized in the nucleus (http://psort.nibb.jp) but does not contain an obvious nuclear localization sequence. Hmg3 carries four potential MAP kinase (Fig. 1B) and two potential protein kinase A phosphorylation sites (http://www.expasy.org/cgi-bin/scanprosite) (Fig. 1B), respectively.

***rop1* is required for mating.** To analyze the cellular functions of these putative transcription factors, we constructed *rop1* and *hmg3* deletion strains. To this end the genes in strains FB1 (*a1 b1*), FB2 (*a2 b2*), and SG200 (*a1*::*mfa2 bE1 bW2*) were replaced with either a hygromycin or nourseothricin resistance cassette (see Materials and Methods for details). The resulting deletion strains were viable, showed no apparent growth defect (not shown), and displayed a budding pattern indistinguishable from that of wild-type strains (see below).

To test for mating, compatible deletion strains were cospotted on PD-charcoal plates. On these plates compatible wild-type strains fuse and form dikaryotic hyphae, which appear as white fuzziness (Fig. 2A). When cospotted with an *a2 b2* wild-type partner, compatible FB1Δrop1 strains displayed slightly attenuated filamentation, while compatible mixtures of an *a1 b1* wild-type strain and FB2Δrop1 strains showed significant reduction in filament formation (Fig. 2A). This might be due to different genetic backgrounds of the *a1 b1* and *a2 b2* strains. However, mixtures of compatible Δ*rop1* strains were unable to develop dikaryotic hyphae (Fig. 2A), indicating that *rop1* is required for successful recognition or fusion with a compatible partner. The Δ*rop1* phenotype could be complemented by introducing the *rop1* gene under the control of the constitutive *otef* promoter into a *rop1* deletion strain (Fig. 2A). In addition, the effects of the *rop1* deletion were studied in the solopathogenic SG200 strain. The SG200 wild-type strain shows filamentous growth on PD-charcoal plates because of autocrine pheromone stimulation and the presence of an active bE/bW heterodimer (Fig. 2B) (5). SG200Δrop1 strains were nonfilamentous (Fig. 2B), which suggests a postfusion role for Rop1.

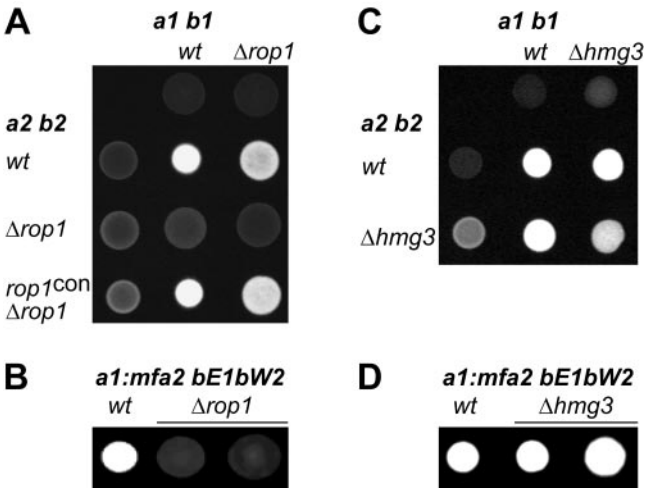

FIG. 2. Mating and filamentation defects of *rop1* and *hmg3* deletion strains. The strains indicated on top are FB1 (*a1 b1*) and SG200 (*a1*::*mfa2 bE1 bW2*) derivatives. Strains indicated to the left are FB2 (*a2 b2*) derivatives. Indicated wild-type (wt) and mutant strains were spotted alone or in combinations on charcoal-containing PD plates. Dikaryotic and *b*-dependent filaments appear as white fuzziness.

The plate mating assay with compatible *hmg3* deletion strains revealed a reduction in dikaryotic filament formation which was only apparent in crosses of compatible Δ*hmg3* strains (Fig. 2C). Filamentation of the solopathogenic SG200Δhmg3 strains was similar to that of the respective wild type (Fig. 2D). This indicates minor defects in cell fusion of *hmg3* deletion strains.

***rop1* is essential for conjugation tube formation upon pheromone stimulation, while *hmg3* is not.** To examine the roles of these two HMG box proteins in the pheromone signaling pathway, we tested the deletion strains for their ability to form conjugation hyphae upon stimulation with synthetic pheromone (47). When stimulated with pheromone, wild-type cells

FIG. 1. *U. maydis* genome contains three sequence-specific HMG domain proteins. (A) Bootstrap analysis (with Clustal X [48] and neighbor-joining plot programs) of the nine HMG domains encoded by the *U. maydis* genome compared to sequence-specific and non-sequence-specific HMG domains of several fungal species. Amino acid positions in the proteins are given as lowercase numbers. $ABF2_{43–111}$ (*S. cerevisiae*, accession no. sp|Q02486), $Cmb1_{141–220}$ (*S. pombe*, accession no. sp|Q10241), $NHP6A_{21–89}$ (*S. cerevisiae*, accession no. sp|P11632), $FPR11_{69–237}$ (*Podospora anserina*, accession no. sp|P35693) $Mta\text{-}1_{116–184}$ (*Neurospora crassa*, accession no. sp|P36981), Mat2 (*Gibberella fujikuroi*; accession no. dbj|BAA75905.1), $Mat1\text{-}Mc_{103-171}$ (*S. pombe*, accession no. sp|P10840), $Pcc1_{24–98}$ (*C. cinereus*, dbj BAA33018.1), $Ste11_{16–80}$ (*S. pombe*, accession no. sp|P36631), $ROX1_{10–83}$ (*S. cerevisiae*, accession no. sp|P25042), and $Mat1\text{-}2_{129–203}$ (*C. heterostrophus*, accession no. pir|S34811). The HMG domains of $Prf1_{126–197}$ (accession no. gb|AAC32736), $Rop1_{215–295}$ (accession no. gb|AY677184), and $Hmg3_{57–140}$ (accession no. gb|AY677183) cluster with the sequence-specific class, whereas the other six *Ustilago* HMG domains given as annotation codes (http://mips.gsf.de/genre/proj/ustilago) appear in the non-sequence-specific class. (B) Schematic representation of *U. maydis* Rop1, Prf1, and Hmg3 domain structure. Features were identified with the PrositeScan and PSORT engines. Putative MAP kinase (diamonds) and protein kinase A (grey ellipses) phosphorylation sites are shown; numbers above the line indicate MAP kinase phosphorylation sites, and numbers below protein kinase A phosphorylation sites. The HMG domains are represented by open rectangles, and the potential nuclear localization sequences (NLS) are depicted as black ellipsoids. The numbers on the right indicate the sizes of the proteins in amino acids.

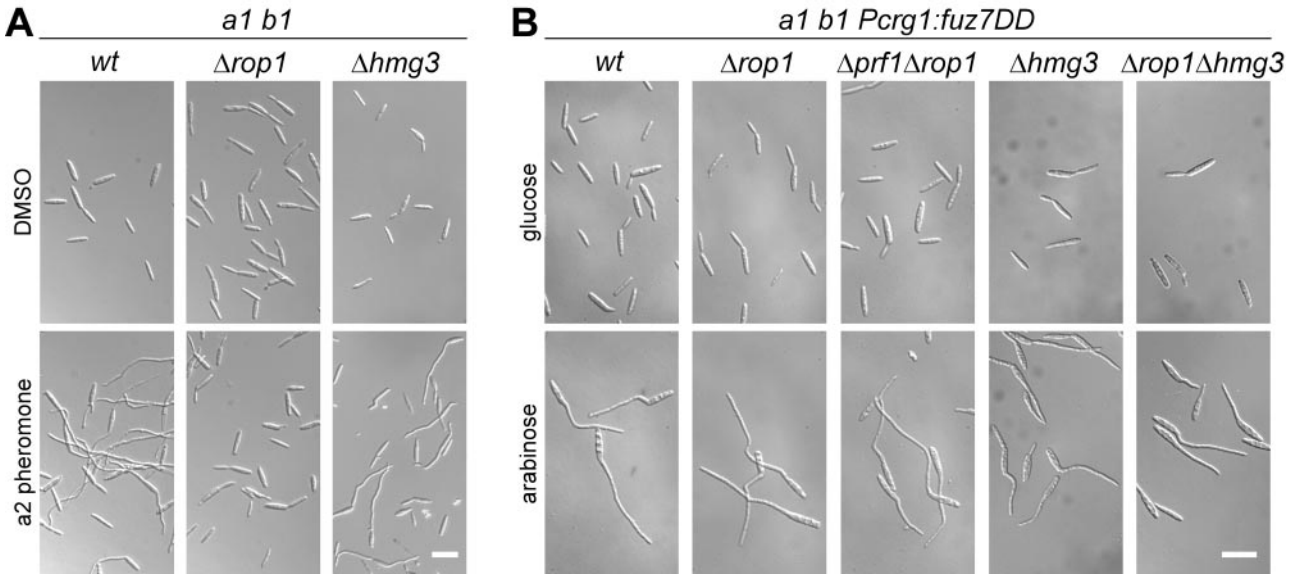

FIG. 3. Influence of *rop1* and *hmg3* deletions on conjugation tube formation. (A) The FB1 (*a1 b1*) wild-type (wt) and mutant strains indicated on top were stimulated with a2 pheromone for 5 h (lower panel) or treated with dimethyl sulfoxide for the same period of time (upper panel). All pictures were taken at the same magnification. Bar, 20 μm. (B) All strains indicated on top are derivatives of FB1Pcrg1::fuz7DD, encoding an arabinose-inducible, constitutively active allele of the MAPKK Fuz7. Cell morphology after 5 h in arabinose-containing medium (lower panels) was compared to that of cells grown with glucose as the carbon source for the same period of time (upper panels). All pictures were taken at the same magnification. Bar, 20 μm.

react with the formation of conjugation hyphae, and this morphological transition could also be observed with *hmg3* mutant cells (Fig. 3A). In contrast, pheromone-stimulated Δ*rop1* cells were unable to form conjugation hyphae (Fig. 3A). On these grounds, we concentrated on further characterization of *rop1*, which is essential for conjugation tube formation.

Overexpression of the constitutively active MAPKK Fuz7DD leads to the formation of conjugation tubes in *rop1* deletion strains. The observed phenotypes of *rop1* mutants could be due to defects upstream or downstream of the MAP kinase cascade, which is involved in transmitting the pheromone signal. To analyze this, we deleted *rop1* in a strain coding for a constitutively active allele of the MAPKK *fuz7* (*fuz7DD*) under the control of the arabinose-inducible *crg1* promoter. The arabinose-induced FB1Pcrg1::fuz7DDΔrop1 strain developed conjugation tubes as efficiently as the progenitor strain (Fig. 3B). This makes it unlikely that Rop1 is the transcription factor regulating conjugation tube formation downstream of the MAP kinase cascade.

To check for redundant functions of Rop1, Hmg3, and Prf1 in this process, we examined Δ*prf1* Δ*rop1* and Δ*rop1* Δ*hmg3* double mutants. Again, arabinose induction of *fuz7DD* resulted in efficient formation of conjugation hyphae in these strains (Fig. 3B), making it unlikely that these transcription factors can substitute for each other.

Rop1 is essential for pheromone-responsive gene expression. To further dissect the role of *rop1* during mating, we performed Northern analyses of *prf1*, *pra1*, *mfa1*, *bE*, and *bW* after pheromone treatment of *rop1* mutant and wild-type cells as controls (Fig. 4). As shown before (51) the pheromone-responsive genes *prf1*, *bE1*, *W1*, *pra1*, and *mfa1* showed a basal level of expression (Fig. 4A, lanes 1 and 3) which was strongly induced upon stimulation with compatible pheromone (Fig. 4A, lane 4). In contrast, in *rop1* mutants, neither basal nor pheromone-induced transcription of these genes could be detected (Fig. 4A, lanes 5 and 6).

We also analyzed expression of these genes in a strain carrying the arabinose-inducible constitutively active allele of *fuz7* (*fuz7DD*). Again, *rop1* was required for basal as well as induced expression of *mfa1* and *prf1* under these conditions (Fig. 4B, lanes 7 and 8). Since deletion of *rop1* affects the transcription of several genes regulated by Prf1, *rop1* is most likely essential for the expression of the pheromone response factor *prf1*. This observation also suggests that *rop1* acts downstream of the Kpp2 MAP kinase cascade. Alternatively, Rop1 could lie in a parallel pathway feeding into *prf1* gene transcription.

Regulation of *rop1* gene expression. Northern analyses of *rop1* gene expression in haploid cells revealed the presence of three *rop1* transcripts of different sizes. Whereas the amounts and ratios of these transcripts remained unaffected by pheromone stimulation (Fig. 4A, lanes 3 and 4), the expression of the constitutively active MAPKK Fuz7DD induced the disappearance of the larger transcript (Fig. 4B, lanes 1 and 2) and enhanced the amounts of the smallest *rop1* transcript (Fig. 4B, lanes 1 and 2). Moreover, the MAP kinase Kpp2 was required for the accumulation of all *rop1* transcripts (Fig. 4B, lanes 3 and 4), while deletion of *prf1* did not affect the amounts and ratios of the *rop1* transcripts (Fig. 4B, lanes 6 and 7). This demonstrates that *kpp2* but not *prf1* is involved in the transcriptional regulation of *rop1*.

To rule out the possibility that the MAP kinase Kpp6 (9) represses *rop1* gene expression in the absence of Kpp2 protein, we have analyzed *rop1* transcript levels under conditions where the MAP kinase module was genetically activated in the presence of either wild-type Kpp2 or the unphosphorylatable Kpp2AEF version (37). In the strain expressing Kpp2AEF,

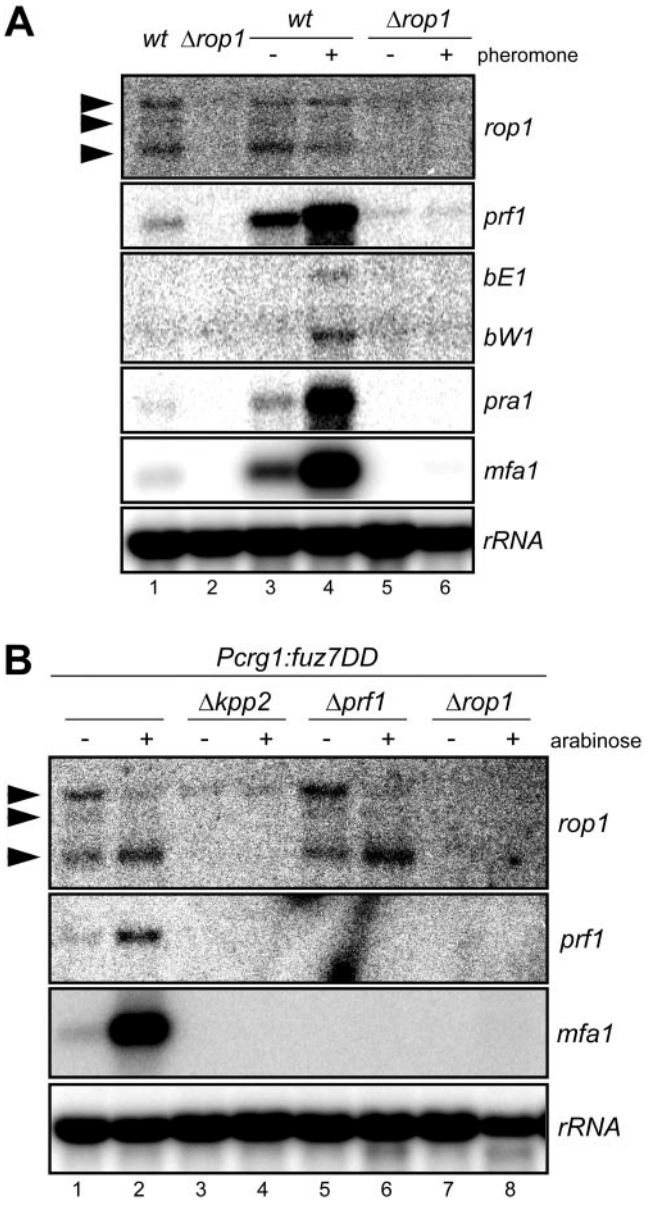

FIG. 4. *rop1* is required for pheromone-responsive gene expression. RNA was prepared from the strains listed on top and subjected to Northern analysis. (A) All strains indicated on top are FB1 (*a1 b1*) derivatives. Cells were either untreated (lanes 1 and 2) or treated for 5 h with synthetic a2 pheromone dissolved in dimethyl sulfoxide (+) or with the same volume of dimethyl sulfoxide (−) (lanes 3 to 6); 10 μg of total RNA was loaded per lane. The blot was probed successively with the gene probes indicated on the right. (B) All strains used are derivatives of strain FB1Pcrg1::fuz7DD. Strains were grown with glucose (−) or arabinose (+) as the carbon source. RNA was isolated, and 12 μg of total RNA was loaded per lane. The filter was hybridized in succession with the gene probes indicated on the right. The rRNA probe served as a loading control. Arrowheads mark the three *rop1* transcripts.

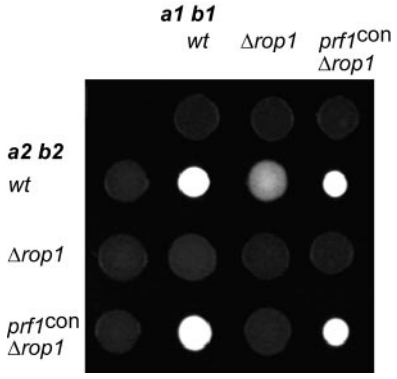

FIG. 5. Constitutive expression of *prf1* restores mating of *rop1* deletion strains. The strains indicated on top are FB1 (*a1 b1*) derivatives. Strains indicated to the left are FB2 (*a2 b2*) derivatives. The indicated wild-type (wt) and mutant strains were spotted alone or in combinations on charcoal-containing PD plates. Dikaryotic filaments appear as white fuzziness.

significantly lower levels of *rop1* transcripts were detected (not shown; H. Eichhorn and R. Kahmann, unpublished). This illustrates that a functional Kpp2 protein is required for *rop1* expression. Since the *rop1* gene contains two introns of 462 and 441 bp in its 5′ region, we considered the larger transcripts to be unspliced variants. Some hints that would support this notion came from the sequencing of 5′- and 3′-rapid amplification of cDNA ends (RACE) products (data not shown). 5′-RACE experiments revealed the existence of four RNA species corresponding to unspliced, spliced for either the first or second intron, or spliced at both introns (not shown). 3′-RACE with an oligo(dT) primer amplified only the *rop1*-specific product without introns, indicating that the unspliced or partially spliced *rop1* RNAs are not polyadenylated (not shown). Taken together, these data indicate that the MAP kinase module is required for *rop1* expression as well as for correct processing of the *rop1* message.

Δ*rop1* defects are complemented by constitutive expression of *prf1*. To substantiate the assertion that the observed phenotypes of *rop1* mutants are due to the insufficient expression of *prf1* we replaced the native *prf1* promoter with the constitutive *tef* promoter in the Δ*rop1* background. The constitutive expression of *prf1* in compatible *rop1* deletion strains restored mating on charcoal (Fig. 5), indicating that Rop1 is an important regulator of *prf1*.

The *prf1* promoter is subject to complex transcriptional regulation. On the one hand it is autoregulated by Prf1 itself via the pheromone response elements (PREs) in the proximal part of the promoter (18). On the other hand *prf1* gene expression is subject to nutritional signaling via the upstream activating sequence (UAS) in the distal part of the promoter (19). To assay whether *rop1* acts via the UAS, we deleted *rop1* in HA232. This strain carries a *gfp* reporter gene under the control of a triple repeat of the UAS (19). As shown before, UAS reporter gene activity is highly induced in cells grown in NM with glucose compared to cells grown in NM with maltose (19) (Table 2). Since the expression levels of the reporter gene were comparable in the *rop1* deletion strain (Table 2), *rop1* does not regulate *prf1* transcription via the UAS.

Rop1 protein binds the *prf1* promoter specifically. To analyze whether Rop1 directly regulates *prf1* gene expression via elements in the *prf1* promoter, we examined heterologously expressed His-tagged versions of Rop1 and Prf1 proteins com-

TABLE 2. Influence of *rop1* deletion on UAS activity and pheromone induction of the *prf1* promoter

Strain	Relative fluorescence[a] (±SEM)			
	NM-glucose	NM-maltose	Control	Pheromone
HA232	1.00 (±0.09)	0.13 (±0.02)	ND	ND
HA232Δrop1	0.98 (±0.07)	0.15 (±0.02)	ND	ND
FB1P_{prf1}:gfp	ND	ND	1.00 (±0.03)	36.02 (±0.34)
FB1Δrop1P_{prf1}:gfp	ND	ND	0.19 (±0.03)	0.11 (±0.02)
FB2P_{prf1}:gfp	ND	ND	1.00 (±0.10)	13.28 (±0.09)
FB2Δrop1P_{prf1}:gfp	ND	ND	0.45 (±0.19)	0.40 (±0.06)

[a] Relative fluorescence was calculated from measured GFP fluorescence per OD_{600}. The average relative fluorescence of the wild-type strains (HA232, FB1Pprf1:gfp, and FB2Pprf1:gfp) grown in glucose-containing medium or treated with dimethyl sulfoxide (control) was set to 1.

prising the HMG domains ($Rop1_{100–401}$ and $Prf1_{1–289}$ respectively) in electrophoretic mobility shift assays (Fig. 6). Under the binding conditions used, $Prf1_{1–289}$ binds to the PRE-containing fragment d (Fig. 6B, lane 12) and shows weak interactions with fragments a and e (Fig. 6B, lanes 3 and 15). The latter can be explained by the presence of PRE-related elements in these fragments.

To map the binding sites more precisely, fragments a and d were digested into two overlapping fragments and used in electrophoretic mobility shift assays (Fig. 6C). Again, $Prf1_{1–289}$ only showed significant interaction with the PRE-containing fragment d1 (Fig. 6C, lane 9). Under the same conditions, purified $Rop1_{100–401}$ showed strong binding to *prf1* promoter fragments a and d (Fig. 6B, lanes 2 and 11), whereas for fragments b, c, and e only very weak interactions could be observed (Fig. 6B, lanes 5, 8, and 14). To delineate the Rop1 recognition site, the high-affinity-binding fragments a and d were digested into two overlapping fragments and used in electrophoretic mobility shift assays (Fig. 6C). This experiment revealed a strong specific interaction of $Rop1_{100–401}$ with fragments a1 and d2 (Fig. 6C, lanes 2 and 11), while the interaction with fragment d1 was only weak (Fig. 6C, lane 8).

A comparison of the DNA sequences of fragments a1 (without the a2 overlap) and d2 led to the identification of three nearly identical sequence stretches of 11 bp with the consensus ATTGT(T/C)(C/T)T(A/T)TC with significant similarities to binding sites of other sequence-specific HMG domain proteins (Fig. 6A). This motif is exclusively present in the $Rop1_{100–401}$ binding fragments of the *prf1* promoter (Fig. 6A, fragments a and d), which made it a good candidate for a Rop1 recognition site (RRS). To test this directly, synthetic double-stranded oligonucleotides comprising one of the three putative RRS sequences were tested in electrophoretic mobility shift assays. Indeed, $Rop1_{100–401}$ showed a high affinity for all three oligonucleotides, whereas Prf1 did not (Fig. 6D, data shown for RRS2, lanes 2 and 15).

To demonstrate specificity of the DNA-protein interactions, we performed competition experiments by adding increasing amounts of unlabeled oligonucleotides comprising either the PRE box (TCCCTTTGT), the RRS2 element (ATTGTCCTT TC), or a mutagenized RRS motif (RRSm; CGGTGGAGC GA). The retarded Rop1 RRS2 complex was competed efficiently with a 10-fold molar excess of RRS2 oligonucleotide (Fig. 6D, lanes 3 to 6), while a 100-fold molar excess of the PRE oligonucleotide was required for significant competition (Fig. 6D, lanes 7 to 10). As expected for a sequence-specific interaction, the RRSm oligonucleotide containing the mutagenized RRS motif showed no competition at all (Fig. 6D, lanes 11 to 14). This demonstrates that $Rop1_{100–401}$ protein binds sequence-specifically to the RRS motif in vitro. In addition, $Rop1_{100–401}$ showed a very weak affinity for the related PRE box (Fig. 6E, lane 1). This serves to explain the weak interaction of $Rop1_{100–401}$ protein with the *prf1* promoter fragment d1 containing two PRE boxes (Fig. 6C, lane 8). On the other hand, only the PRE (Fig. 6E, lanes 4 to 7) but not the RRS2 (Fig. 6E, lanes 8 to 11) or the RRSm oligonucleotide (Fig. 6E, lanes 12 to 15) was efficient in competing with Prf1 binding to the labeled PRE oligonucleotide (Fig. 6E). Taken together, these results demonstrate that the HMG domains of Rop1 and Prf1 recognize distinct elements in the *prf1* promoter.

***rop1* deletion strains are fully pathogenic.** To analyze the role of *rop1* during pathogenic development, we performed plant infections with crosses of compatible *rop1* deletion strains. As *prf1* deletion strains are nonpathogenic and *rop1* is essential for *prf1* gene expression, we were surprised to observe disease symptoms with compatible Δ*rop1* strains which were as severe as symptoms induced by wild-type strains (Table 3). This result suggests that *rop1* is dispensable for *prf1* gene expression during infection.

To monitor *prf1* gene expression during axenic and pathogenic growth, compatible wild-type and *rop1* deletion strains encoding a *gfp*-reporter gene under the control of the *prf1* promoter were generated. The resulting haploid strains were first analyzed for *gfp* expression after treatment with pheromone or the solvent dimethyl sulfoxide as a control (Fig. 7A). The wild-type strains showed weak basal fluorescence and formed brightly fluorescent conjugation hyphae upon pheromone stimulation. The *rop1* deletion strains did not form conjugation hyphae, and no GFP fluorescence was detectable (Fig. 7A). Moreover, the expression levels of the *Pprf1*::*gfp* reporter were quantified by fluorimetric measurement. This revealed a 13-fold induction in FB2 treated with a1 pheromone and a 36-fold induction in FB1 treated with a2 pheromone (Table 2).

In Δ*rop1* strains, basal expression of the reporter gene was reduced twofold and fivefold in the FB2- and FB1-derived strains, respectively, and pheromone treatment did not elicit an increase in *Pprf1*::*gfp* expression (Table 2). These results confirmed the Northern data on *prf1* gene expression (Fig. 4A, lanes 3 to 6). To monitor *gfp* expression during mating conditions in axenic culture, mixtures of FB1Pprf1::gfp and

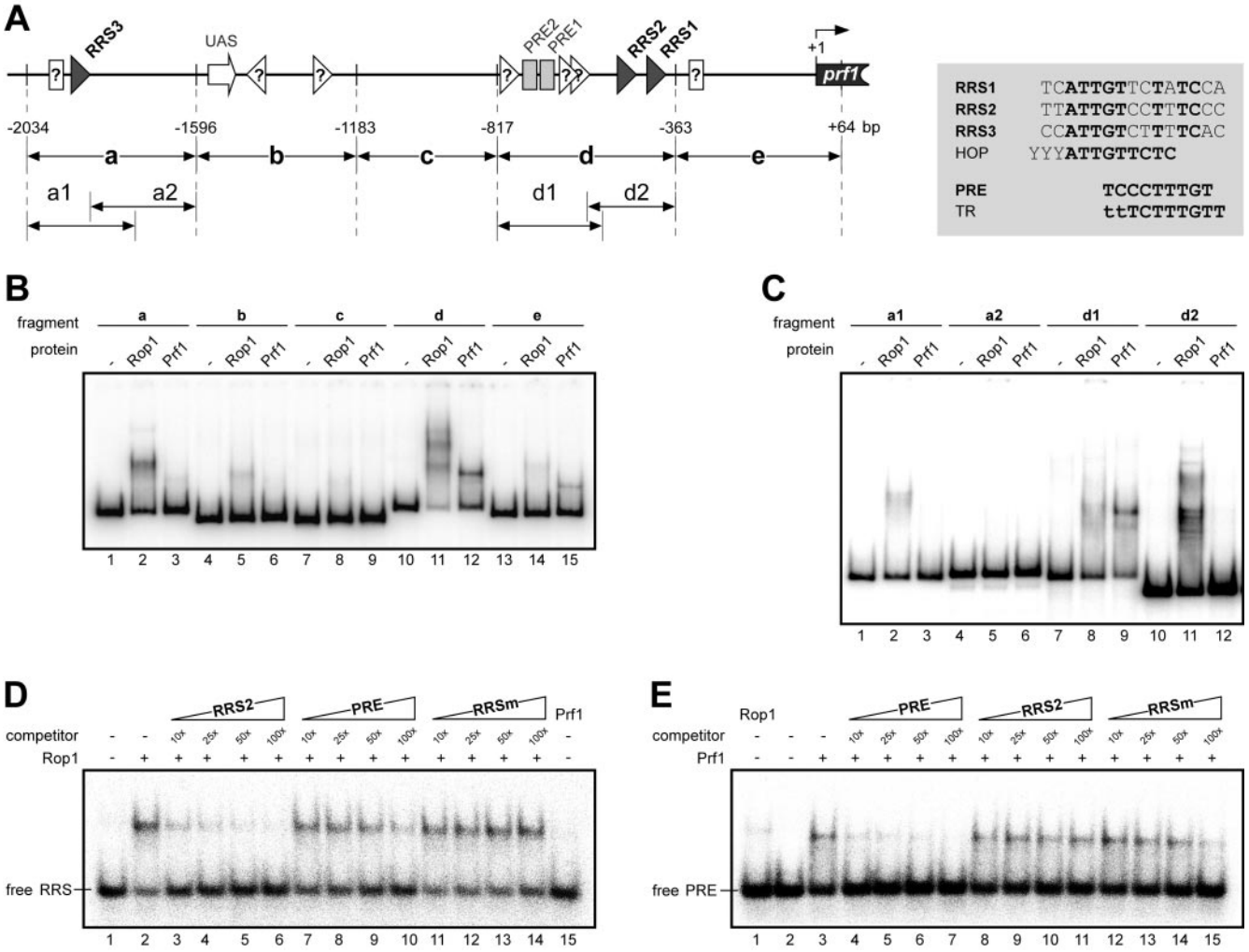

FIG. 6. Rop1 binds to specific sequences in the *prf1* promoter in vitro. (A) Schematic representation of the *prf1* promoter. The UAS is indicated as an open arrow, RRS sequences are depicted as black triangles, and open triangles denote putative additional RRS motifs as suggested by sequence similarity and electrophoretic mobility shift assays. PRE elements are indicated as light grey rectangles, open rectangles denote putative additional PRE elements as suggested by sequence similarity and electrophoretic mobility shift assays. Numbers below indicate positions relative to the ATG. Promoter fragments used in electrophoretic mobility shift assays are indicated as arrows below the scheme. The inset to the right gives the sequences of the three RRS sites identified. Bases present in all three RRS motifs are given in bold. For comparison, the PRE box, a half site of the hypoxic operator (HOP) recognized by Rox1p in *S. cerevisiae*, and the TR element recognized by Ste11 in *S. pombe* are shown. (B to E) Electrophoretic mobility shift assays with His-tagged HMG domains of Rop1 and Prf1 protein with (B) *prf1* promoter fragments a to e and (C) *prf1* promoter fragments a1 and a2 and d1 and d2. (D) Interaction of the Rop1 HMG domain with labeled RRS2 oligonucleotide was analyzed in the presence of increasing amounts (given as fold molar excesses) of the different unlabeled competitors indicated above the lanes. In lane 15, binding of the Prf1 HMG domain to the RRS2 probe was tested in the absence of competitor. (E) Interaction of the Prf1 HMG domain with labeled PRE oligonucleotide was analyzed in the presence of increasing amounts (given as fold molar excess) of the different unlabeled competitors indicated above the lanes. Binding of the Rop1 HMG domain to the PRE probe was tested in the absence of any competitor (lane 1).

FB2Pprf1::gfp as well as FB1Δrop1Pprf1::gfp and FB2Δrop1 Pprf1::gfp were cospotted on PD-charcoal plates for 24 h and 48 h at 28°C and then subjected to microscopic analysis. While the wild-type strains efficiently formed dikaryotic hyphae which showed strong GFP fluorescence (Fig. 7B), not a single mating event or dikaryon could be observed in mixtures of Δ*rop1* strains, and the budding cells displayed little or no GFP fluorescence (Fig. 7B). These findings underscore that *rop1* is essential for *prf1* gene expression during axenic growth. However, when the same strain combinations were used to infect plants, conjugation hyphae, dikaryotic filaments, and appressorium-like structures could be detected in wild-type (Fig. 7C) as well as Δ*rop1* derivatives (Fig. 7D). In addition, GFP fluorescence was visible in all these structures (Fig. 7C and D). This demonstrates that the *prf1* gene is expressed in the plant environment even in the absence of *rop1*.

TABLE 3. Pathogenicity of *rop1* deletion strains

Strain or cross	No. of plants infected	No. of plants with tumors	% with tumors
FB1 × FB2	31	29	94
FB1Δrop1 × FB2Δrop1	65	61	94
SG200	24	23	96
SG200Δrop1	44	41	93

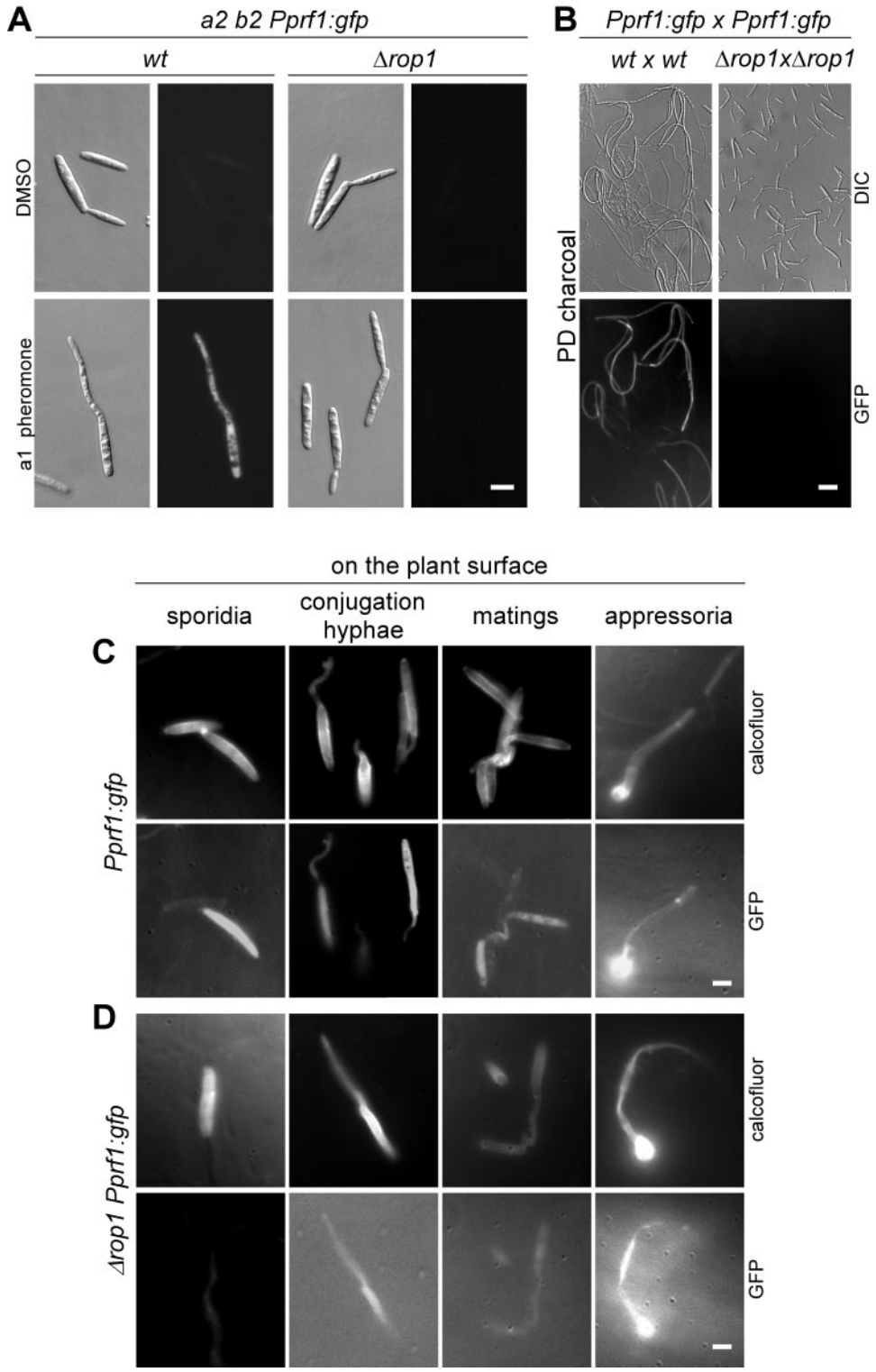

FIG. 7. *rop1* is dispensable for *prf1* gene expression and fungal development on the plant surface. All strains carried one copy of a transcriptional *prf1* promoter-*gfp* fusion (P*prf1*::*gfp)* integrated into the *ip* locus. (A) The FB2 (*a2 b2*)-derived strains are indicated on top; they were stimulated with compatible a1 pheromone for 5 h (lower panel) or treated with dimethyl sulfoxide for the same period of time (upper panel). The right panels show GFP fluorescence of the same cells depicted on the left. All pictures were taken with the same magnification. Bar, 4 μm. (B) Mixtures of compatible wild-type (wt) or compatible Δ*rop1* strains carrying the reporter (P*prf1*::*gfp)* were spotted on charcoal-containing PD plates. The cell mixtures indicated on top were microscoped after 1 day of incubation. Lower panels show GFP fluorescence of the differential interference contrast-visualized cells depicted in the upper panels. All pictures were taken at the same magnification. Bar, 20 μm. (C and D) Mixtures of compatible strains at various stages of development (sporidia, conjugation hyphae, matings, and appressoria) on the plant surface. (C) Wild-type strains. (D) Δ*rop1* mutants. Pictures were taken as indicated on the right with a DAPI filter after Calcofluor staining (upper panels) or a GFP filter to visualize reporter gene expression (lower panels). All pictures were taken at the same magnification. Bar, 4 μm.

DISCUSSION

In this study we have identified two additional sequence-specific HMG box proteins, Rop1 and Hmg3, of which Rop1 was further analyzed. We provide evidence that *rop1* is an essential regulator for *prf1* gene expression during mating in axenic culture. Epistasis analyses positioned *rop1* downstream of the Kpp2 MAP kinase cascade, and in vitro data showed that Rop1 binds specifically to the *prf1* promoter. Despite the crucial role of Rop1 for *prf1* transcription during growth in culture, *rop1* proved dispensable for *prf1* gene expression on the plant surface.

HMG domain proteins as developmental regulators in fungi. The two additional transcription factors, Rop1 and Hmg3, identified in this study belong to the sequence-specific DNA binding class of HMG domain proteins. We demonstrate that *rop1* is essential for basal and induced expression of *prf1*, and this explains all phenotypes of the *rop1* deletion strains associated with mating, pheromone-responsive gene expression, and dikaryon formation during axenic growth. The observation that constitutive expression of *prf1* complements the mating defect of *rop1* deletion strains reinforces the notion that Rop1 is a transcriptional activator for *prf1*, and this was further substantiated by demonstrating direct binding to the *prf1* promoter (see below). Therefore, we conclude that Rop1 directly activates the transcription of *prf1*.

A similar situation exists in *Schizosaccharomyces pombe*, where the HMG domain protein Ste11 (45, 46) directly activates the expression of *mat1-mc*. *mat1-mc* also encodes a sequence-specific HMG domain protein which acts as a transcriptional activator of M-cell-specific genes required for mating, sporulation, and meiosis (25, 27). In contrast to *rop1* deletion strains, Δ*hmg3* strains were only slightly impaired in cell fusion, and it is presently unclear which component of the fusion machinery is affected in these strains. The finding that neither *rop1* nor *hmg3* nor *prf1* (37) is required for conjugation tube formation when this pathway is genetically activated by expressing the constitutively active MAPKK Fuz7DD argues against an involvement of sequence-specific HMG domain proteins as mediators of this morphological transition.

Rop1 target sites. The *prf1* promoter has previously been shown to underlie a complex regulation. While the PREs in the proximal part of the *prf1* promoter most likely confer autoregulation through the *prf1* gene product itself, the distal UAS has been shown to be essential for the transcription of *prf1* and is subject to nutritional regulation (19). As *rop1* deletion strains show the same level of UAS::*gfp* reporter gene expression as the wild-type strain HA232, we conclude that Rop1 does not regulate *prf1* gene expression via the UAS. Instead, electrophoretic mobility shift assays combined with quantitative competition experiments applying specific and unspecific oligonucleotides demonstrate that the Rop1 HMG domain specifically binds to RRS elements in the *prf1* promoter. The RRS element (consensus: ATTGT[C/T][C/T]T[A/T]TC) is distinct from the PRE boxes (consensus: TCCCTTTGT) and is not recognized by the HMG domain of Prf1. For the two HMG domain proteins Ste11 and Mat1-Mc of *S. pombe*, it has been demonstrated that they both bind the TR element (consensus: ttTCTTTGTT) with approximately the same affinity (27).

When compared with the RRS motif sequence, similarity is most prominent in the 3′ portion. The 5′ portion of the RRS shows striking similarity to the motif YYYATTGTTCTC, which is recognized by Rox1p, the sole sequence-specific HMG domain protein in *S. cerevisiae* (2). In contrast to Rop1, which acts as an activator of *prf1* expression, Rox1p functions as a repressor for genes required during oxygen limitation (57). Interestingly, in the human pathogen *C. albicans* the HMG domain protein Rfg1, which recognizes the same sequence element as Rox1p in *S. cerevisiae*, is not involved in the response to low oxygen but controls hyphal growth (26). The Rop1 binding RRS motif identified in this study is also found in a number of other promoter regions in *U. maydis*. This implicates Rop1 in the transcriptional regulation of a variety of other genes besides *prf1*. The fact that we were unable to detect additional phenotypes except the effects on *prf1* may indicate that the expression of this set of genes is not relevant under the culture conditions applied.

Regulation of *rop1* gene expression and protein activity. The observation that *rop1* is essential for *prf1* and pheromone-responsive gene expression in strains with a genetically activated MAP kinase cascade makes it likely that *rop1* functions downstream of the MAP kinase Kpp2. This notion is supported by the observation that *rop1* gene expression is regulated by this pathway. Of the three *rop1* transcripts detected by Northern blot, only the smallest appears to be polyadenylated and completely spliced and is therefore likely to represent mature *rop1* mRNA. In *kpp2* deletion strains, the induction of *fuz7DD* by the shift from glucose to arabinose medium does not allow us to detect spliced *rop1* transcripts, while these are readily detectable when the same experiment is done in the presence of Kpp2. This rules out that the shift to arabinose-containing medium is promoting the processing of *rop1* message and implicates Kpp2 in the generation of these spliced transcripts. How this is achieved is presently unknown. However, precedence for a role of a MAP kinase module in splicing exists. In human cell lines, alternative splicing of CD44 pre-mRNA is regulated via phosphorylation of the RNA-binding protein Sam68 by the ERK kinase (34, 54).

The presence of potential MAP kinase phosphorylation sites in Rop1 may indicate that Kpp2 is not only involved in generating the mature *rop1* transcript but may also affect the activity of Rop1 protein.

Rop1 is a critical factor for the regulation of *prf1*. While Rop1 is a critical factor for the regulation of *prf1* during mating and dikaryon formation in axenic culture, *rop1* is dispensable for pathogenic development. This came as a surprise because *prf1* is not only essential during mating in axenic culture but also crucial for mating on the leaf surface and subsequent pathogenic development (18). This implies that on the leaf surface, *prf1* gene expression must be induced by the perception of an as yet unidentified environmental signal not present during axenic growth. In the phytopathogenic fungi *M. grisea*, *Colletotrichum gloeosporioides*, and *Uromyces appendiculatus*, surface hydrophobicity and leaf topography, plant hormones, and wax components have been reported to be perceived and to induce appressorial differentiation (28, 50).

In *U. maydis* there is no evidence that hydrophobicity alone is sufficient to stimulate *prf1* gene expression in the absence of *rop1* (T. Brefort, unpublished data), which could indicate that chemical rather than physical signals serve as major stimuli. In

any case, the signal must bypass the need for *rop1*. This points to the existence of an as yet unidentified transcription factor with an essential role in *prf1* expression during fungal growth on the plant surface. The transmission of the postulated environmental signal might occur via the described cAMP or MAP kinase pathways (37) or an additional pathway acting in parallel. In this scenario, the UAS-mediated regulation of *prf1* gene expression could be important. Interestingly, the IME2-like MAP kinase Crk1 was recently described to regulate *prf1* expression via the UAS (14, 15). It is thus conceivable that Crk1 might be responsible for activation of the unknown transcription factor acting via the UAS. We are currently trying to isolate the regulator that promotes *prf1* transcription through the UAS to sort out the complex mode of regulation affecting the *prf1* promoter.

ACKNOWLEDGMENTS

Our work was supported by the German Science Foundation (DFG) through grant SFB369 and by BayerCropScience AG.

REFERENCES

1. **Andrews, D. L., J. D. Egan, M. E. Mayorga, and S. E. Gold.** 2000. The *Ustilago maydis ubc4* and *ubc5* genes encode members of a MAP kinase cascade required for filamentous growth. Mol. Plant-Microbe Interact. 1**3:** 781–786.
2. **Balasubramanian, B., C. V. Lowry, and R. S. Zitomer.** 1993. The Rox1 repressor of the *Saccharomyces cerevisiae* hypoxic genes is a specific DNA-binding protein with a high-mobility group motif. Mol. Cell. Biol. 1**3:**6071–6078.
3. **Banuett, F., and I. Herskowitz.** 1989. Different a-Alleles are necessary for maintenance of filamentous growth but not for meiosis. Proc. Natl. Acad. Sci. USA **86:**5878–5882.
4. **Banuett, F., and I. Herskowitz.** 1994. Identification of *fuz7*, a *Ustilago maydis* MEK/MAPKK homolog required for a-locus-dependent and -independent steps in the fungal life cycle. Genes Dev. **8:**1367–1378.
5. **Bolker, M., H. U. Bohnert, K. H. Braun, J. Gorl, and R. Kahmann.** 1995. Tagging pathogenicity genes in *Ustilago maydis* by restriction enzyme-mediated integration (REMI). Mol. Gen. Genet. 2 **48:**547–552.
6. **Bolker, M., M. Urban, and R. Kahmann.** 1992. The *a* mating type locus of *U. maydis* specifies cell signaling components. Cell **68:**441–450.
7. **Bottin, A., J. Kamper, and R. Kahmann.** 1996. Isolation of a carbon source-regulated gene from *Ustilago maydis*. Mol. Gen. Genet. 2**53:**342–352.
8. **Brachmann, A., J. Konig, C. Julius, and M. Feldbrugge.** 2004. A reverse genetic approach for generating gene replacement mutants in *Ustilago maydis*. Mol. Genet. Genomics **272:**216–226.
9. **Brachmann, A., J. Schirawski, P. Muller, and R. Kahmann.** 2003. An unusual MAP kinase is required for efficient penetration of the plant surface by *Ustilago maydis*. EMBO J. **22:**2199–2210.
10. **Brachmann, A., G. Weinzierl, J. Kamper, and R. Kahmann.** 2001. Identification of genes in the bW/bE regulatory cascade in *Ustilago maydis*. Mol. Microbiol. **42:**1047–1063.
11. **Bustin, M., and R. Reeves.** 1996. High-mobility-group chromosomal proteins: architectural components that facilitate chromatin function. Prog. Nucleic Acid Res. Mol. Biol. **54:**35–100.
12. **Chang, Y. C., L. A. Penoyer, and K. J. Kwon-Chung.** 2001. The second STE12 homologue of *Cryptococcus neoformans* is MATa-specific and plays an important role in virulence. Proc. Natl. Acad. Sci. USA **98:**3258–3263.
13. **Clark-Lewis, I., J. S. Sanghera, and S. L. Pelech.** 1991. Definition of a consensus sequence for peptide substrate recognition by p44mpk, the meiosis-activated myelin basic protein kinase. J. Biol. Chem. 2**66:**15180–15184.
14. **Garrido, E., and J. Perez-Martin.** 2003. The *crk1* gene encodes an Ime2-related protein that is required for morphogenesis in the plant pathogen *Ustilago maydis*. Mol. Microbiol. **47:**729–743.
15. **Garrido, E., U. Voss, P. Muller, R. Kahmann, and J. Pérez-Martín.** 2004. The induction of sexual development and virulence in the smut fungus *Ustilago maydis* depends on Crk1, a novel MAP kinase protein. Genes Dev. **18:**3117–3130.
16. **Gillissen, B., J. Bergemann, C. Sandmann, B. Schroeer, M. Bolker, and R. Kahmann.** 1992. A two-component regulatory system for self/non-self recognition in *Ustilago maydis*. Cell **68:**647–657.
17. **Grosschedl, R., K. Giese, and J. Pagel.** 1994. HMG domain proteins: architectural elements in the assembly of nucleoprotein structures. Trends Genet. 1**0:**94–100.
18. **Hartmann, H. A., R. Kahmann, and M. Bolker.** 1996. The pheromone response factor coordinates filamentous growth and pathogenicity in *Ustilago maydis*. EMBO J. 1**5:**1632–1641.
19. **Hartmann, H. A., J. Kruger, F. Lottspeich, and R. Kahmann.** 1999. Environmental signals controlling sexual development of the corn Smut fungus *Ustilago maydis* through the transcriptional regulator Prf1. Plant Cell **11:** 1293–1306.
20. **Hoffman, C. S., and F. Winston.** 1987. A ten-minute DNA preparation from yeast efficiently releases autonomous plasmids for transformation of *Escherichia coli*. Gene **57:**267–272.
21. **Holliday, R.** 1974. *Ustilago maydis*, p. 575–595. *In* R. C. King (ed.), Handbook of genetics, vol. 1. Plenum Press, New York, N.Y.
22. **Kaffarnik, F., P. Muller, M. Leibundgut, R. Kahmann, and M. Feldbrugge.** 2003. PKA and MAPK phosphorylation of Prf1 allows promoter discrimination in *Ustilago maydis*. EMBO J. **22:**5817–5826.
23. **Kamper, J.** 2004. A PCR-based system for highly efficient generation of gene replacement mutants in *Ustilago maydis* Mol. Genet. Genomics **271:**103–110.
24. **Kamper, J., M. Reichmann, T. Romeis, M. Bolker, and R. Kahmann.** 1995. Multiallelic recognition: non-self-dependent dimerization of the bE and bW homeodomain proteins in *Ustilago maydis*. Cell **81:**73–83.
25. **Kelly, M., J. Burke, M. Smith, A. Klar, and D. Beach.** 1988. Four mating type genes control sexual differentiation in the fission yeast. EMBO J. **7:**1537–1547.
26. **Khalaf, R. A., and R. S. Zitomer.** 2001. The DNA binding protein Rfg1 is a repressor of filamentation in *Candida albicans*. Genetics 1**57:**1503–1512.
27. **Kjaerulff, S., D. Dooijes, H. Clevers, and O. Nielsen.** 1997. Cell differentiation by interaction of two HMG-box proteins: Mat1-Mc activates M cell-specific genes in *S. pombe* by recruiting the ubiquitous transcription factor Ste11 to weak binding sites. EMBO J. 1**6:**4021–4033.
28. **Kolattukudy, P. E., L. M. Rogers, D. Li, C. S. Hwang, and M. A. Flaishman.** 1995. Surface signaling in pathogenesis. Proc. Natl. Acad. Sci. USA **92:**4080–4087.
29. **Kruger, J., G. Loubradou, E. Regenfelder, A. Hartmann, and R. Kahmann.** 1998. Crosstalk between cAMP and pheromone signalling pathways in *Ustilago maydis*. Mol. Gen. Genet. 2**60:**193–198.
30. **Laudet, V., D. Stehelin, and H. Clevers.** 1993. Ancestry and diversity of the HMG box superfamily. Nucleic Acids Res. **21:**2493–2501.
31. **Liu, H., J. Kohler, and G. R. Fink.** 1994. Suppression of hyphal formation in *Candida albicans* by mutation of a STE12 homolog. Science 2**66:**1723–1726.
32. **Lo, H. J., J. R. Kohler, B. DiDomenico, D. Loebenberg, A. Cacciapuoti, and G. R. Fink.** 1997. Nonfilamentous *C. albicans* mutants are avirulent. Cell **90:**939–949.
33. **Loubradou, G., A. Brachmann, M. Feldbrugge, and R. Kahmann.** 2001. A homologue of the transcriptional repressor Ssn6p antagonizes cAMP signalling in *Ustilago maydis*. Mol. Microbiol. **40:**719–730.
34. **Matter, N., P. Herrlich, and H. Konig.** 2002. Signal-dependent regulation of splicing via phosphorylation of Sam68. Nature **420:**691–695.
35. **Mayorga, M. E., and S. E. Gold.** 1999. A MAP kinase encoded by the *ubc3* gene of *Ustilago maydis* is required for filamentous growth and full virulence. Mol. Microbiol. **34:**485–497.
36. **Muller, P., C. Aichinger, M. Feldbrugge, and R. Kahmann.** 1999. The MAP kinase Kpp2 regulates mating and pathogenic development in *Ustilago maydis*. Mol. Microbiol. **34:**1007–1017.
37. **Muller, P., G. Weinzierl, A. Brachmann, M. Feldbrugge, and R. Kahmann.** 2003. Mating and pathogenic development of the smut fungus *Ustilago maydis* are regulated by one mitogen-activated protein kinase cascade. Eukaryot. Cell **2:**1187–1199.
38. **Murata, Y., M. Fujii, M. E. Zolan, and T. Kamada.** 1998. Molecular analysis of *pcc1*, a gene that leads to A-regulated sexual morphogenesis in *Coprinus cinereus*. Genetics 1**49:**1753–1761.
39. **Park, G., C. Xue, L. Zheng, S. Lam, and J. R. Xu.** 2002. MST12 regulates infectious growth but not appressorium formation in the rice blast fungus *Magnaporthe grisea*. Mol. Plant-Microbe Interact. 1**5:**183–192.
40. **Pevny, L. H., and R. LovellBadge.** 1997. Sox genes find their feet. Curr. Opin. Genet. Dev. **7:**338–344.
41. **Regenfelder, E., T. Spellig, A. Hartmann, S. Lauenstein, M. Bolker, and R. Kahmann.** 1997. G proteins in *Ustilago maydis*: transmission of multiple signals? EMBO J. 1**6:**1934–1942.
42. **Sambrook, J., E. F. Fritsch, and T. Maniatis** 1989. Molecular cloning: a laboratory manual, 2nd ed. Cold Spring Harbor Laboratory Press, Cold Spring Harbor, N.Y.
43. **Schulz, B., F. Banuett, M. Dahl, R. Schlesinger, W. Schafer, T. Martin, I. Herskowitz, and R. Kahmann.** 1990. The *b* alleles of *U. maydis*, whose combinations program pathogenic development, code for polypeptides containing a homeodomain-related motif. Cell **60:**295–306.
44. **Sinclair, A. H., P. Berta, M. S. Palmer, J. R. Hawkins, B. L. Griffiths, M. J. Smith, J. W. Foster, A. M. Frischauf, R. Lovell-Badge, and P. N. Goodfellow.** 1990. A gene from the human sex-determining region encodes a protein with homology to a conserved DNA-binding motif. Nature **346:**240–244.
45. **Sipiczki, M.** 1988. The role of sterility genes (*ste* and *aff*) in the initiation of sexual development in *Schizosaccharomyces pombe*. Mol. Gen. Genet. 21**3:** 529–534.
46. **Sugimoto, A., Y. Iino, T. Maeda, Y. Watanabe, and M. Yamamoto.** 1991.

Schizosaccharomyces pombe ste11+ encodes a transcription factor with an HMG motif that is a critical regulator of sexual development. Genes Dev. **5:**1990–1999.

47. **Szabo, Z., M. Tonnis, H. Kessler, and M. Feldbrugge.** 2002. Structure-function analysis of lipopeptide pheromones from the plant pathogen *Ustilago maydis*. Mol. Genet. Genomics 2**68:**362–370.
48. **Thompson, J. D., T. J. Gibson, F. Plewniak, F. Jeanmougin, and D. G. Higgins.** 1997. The CLUSTAL_X-Windows interface: flexible strategies for multiple sequence alignment aided by quality analysis tools. Nucleic Acids Res. 2**5:**4876–4882.
49. **Travis, A., A. Amsterdam, C. Belanger, and R. Grosschedl.** 1991. LEF-1, a gene encoding a lymphoid-specific protein with an HMG domain, regulates T-cell receptor alpha enhancer function. Genes Dev. **5:**880–894.
50. **Tucker, S. L., and N. J. Talbot.** 2001. Surface attachment and pre-penetration stage development by plant pathogenic fungi. Annu. Rev. Phytopathol. **39:**385–417.
51. **Urban, M., R. Kahmann, and M. Bolker.** 1996. Identification of the pheromone response element in *Ustilago maydis*. Mol. Gen. Genet. **251:**31–37.
52. **van de Wetering, M., M. Oosterwegel, D. Dooijes, and H. Clevers.** 1991. Identification and cloning of TCF-1, a T lymphocyte-specific transcription factor containing a sequence-specific HMG box. EMBO J. 1**0:**123–132.
53. **Wedlich-Soldner, R., M. Bolker, R. Kahmann, and G. Steinberg.** 2000. A putative endosomal t-SNARE links exo- and endocytosis in the phytopathogenic fungus *Ustilago maydis*. EMBO J. 1**9:**1974–1986.
54. **Weg-Remers, S., H. Ponta, P. Herrlich, and H. Konig.** 2001. Regulation of alternative pre-mRNA splicing by the ERK MAP-kinase pathway. EMBO J. 2**0:**4194–4203.
55. **Wickes, B. L., U. Edman, and J. C. Edman.** 1997. The *Cryptococcus neoformans* STE12alpha gene: a putative *Saccharomyces cerevisiae* STE12 homologue that is mating type specific. Mol. Microbiol. 2**6:**951–960.
56. **Yue, C., L. M. Cavallo, J. A. Alspaugh, P. Wang, G. M. Cox, J. R. Perfect, and J. Heitman.** 1999. The STE12alpha homolog is required for haploid filamentation but largely dispensable for mating and virulence in *Cryptococcus neoformans*. Genetics 1**53:**1601–1615.
57. **Zitomer, R. S., P. Carrico, and J. Deckert.** 1997. Regulation of hypoxic gene expression in yeast. Kidney Int. **51:**507–513.